

The crossover from strong to weak chaos for nonlinear waves in disordered systems

T.V. Lapyteva,* J.D. Bodyfelt, D.O. Krimer, Ch. Skokos, and S. Flach
*Max Planck Institute for the Physics of Complex Systems,
 Nöthnitzer Straße 38, D-01187 Dresden, Germany*

We observe a crossover from strong to weak chaos in the evolution of multiple site excitations within disordered chains with cubic nonlinearity. Recent studies have shown that Anderson localization is destroyed, and the wave packet spreading is characterized by an asymptotic divergence of the second moment m_2 in time, as $t^{1/3}$. In the present paper, we observe the existence of a qualitatively new dynamical regime in which the second moment spreads even faster (as $t^{1/2}$), with a crossover to the asymptotic $t^{1/3}$ law at larger times. We analyze the peculiarities of these spreading regimes and perform extensive numerical simulations over large times with ensemble averaging. A novel technique of local derivatives on logarithmic scales is developed in order to quantitatively visualize the slow crossover processes.

PACS numbers: 05.45.-a, 05.60.Cd, 63.20.Pw

Wave propagation within random potentials is an interdisciplinary research field applicable to many diverse systems; regardless of their classical or quantum nature, the overall wave behavior provides common ground for understanding transport properties. One such property - theoretically predicted by Anderson [1] and since labeled “Anderson localization” (AL) - is a halt of wave propagation due to exponentially localized normal modes (NMs) of the random potential. The significance of AL has been evidenced in the past decades by a bevy of experimental observation; including optics [2], acoustics [3], microwaves [4], and matter waves [5].

In many experimental situations, AL can be strongly altered by the appearance of nonlinearity within the potential. These nonlinearities can be induced via the nonlinear Kerr effect in disordered photonic lattices [6], or atomic Bose-Einstein condensate interactions (controlled by Feshbach resonances) in optical lattices [7].

The question of the interplay between disorder and nonlinearity - how the two complement, frustrate, or reinforce each other - is thus of strong importance. The theoretical study of AL in random nonlinear lattices has been advanced using several approaches including the studies of transmission [8] and stationary solutions [9]. Recent research in dynamics of wave spreading within nonlinear disordered media focuses on the spatiotemporal evolution of wave packets, debating the asymptotic spreading law against an eventual blockage [10–15]. Previous numerical studies show that the second moment of a wave packet starting from a single site excitation grows as $t^{1/3}$ [14, 15]. However when starting from a distributed single normal mode state, faster growth is reported, though not quantitatively assessed [14–16]. Theoretical expectations range from spreading without limits to a slowdown and restoration of AL. Different spreading characteristics are also claimed to be $t^{2/5}$ [11], $t^{1/3}$ [14, 15], and a two regime case with $t^{1/2}$ and asymptotic $t^{1/3}$ [17]. This letter aims to clarify some of these controversies.

We first show that using estimates for average spacings

and nonlinear frequency shifts, three different evolution regimes can be identified. In particular, in contrast to previous results we obtain a new regime of strong chaos which is accessible by initial multiple site excitations, but **not** by single site excitations. Contrary to previous studies, we perform extensive ensemble averaging over 1000 disorder realizations. As a result, smooth functional dependencies of wave packet characteristics on time are obtained. Using a novel technique of smoothing and local differentiation on logarithmic scales, we are able to observe the fast spreading regime of strong chaos, preceded by the predicted crossover into the asymptotic regime of weak chaos, as argued in [17]. No saturation and slowing down of the spreading process is observed on the longest time scales of observation.

We study two different Hamiltonian models. The first is the one-dimensional disordered nonlinear Schrödinger (DNLS) equation

$$\mathcal{H}_D = \sum_l \epsilon_l |\psi_l|^2 + \frac{\beta}{2} |\psi_l|^4 - (\psi_{l+1} \psi_l^* + \text{c.c.}) \quad (1)$$

in which ϵ_l is the onsite energy chosen uniformly from a $[-W/2, W/2]$ random distribution. By $\partial_t \psi_l = \partial \mathcal{H}_D / \partial (i\psi_l^*)$, the equations of motion are generated:

$$i\partial_t \psi_l = \epsilon_l \psi_l + \beta |\psi_l|^2 \psi_l - \psi_{l+1} - \psi_{l-1}. \quad (2)$$

The second model considered is oscillators on a quartic Klein-Gordon (KG) lattice, given as

$$\mathcal{H}_K = \sum_l \frac{p_l^2}{2} + \frac{\tilde{\epsilon}_l}{2} u_l^2 + \frac{1}{4} u_l^4 + \frac{1}{2W} (u_{l+1} - u_l)^2 \quad (3)$$

where u_l and p_l are respectively the generalized coordinate/momentum on the site l , and $\tilde{\epsilon}_l$ are the disordered potential strengths chosen uniformly in $[1/2, 3/2]$. Likewise, $\partial_t^2 u_l = -\partial \mathcal{H}_K / \partial u_l$ generates the equations of motion

$$\partial_t^2 u_l = -\tilde{\epsilon}_l u_l - u_l^3 + \frac{1}{W} (u_{l+1} + u_{l-1} - 2u_l). \quad (4)$$

Consider densities of: norm, $n_l = |\psi_l|^2$, for DNLS and individual oscillator energy, \mathcal{E}_l , for KG. In the KG model the total energy, $E = \sum_l \mathcal{E}_l \geq 0$, acts as the nonlinear control parameter, similar to β for the DNLS case. Both models conserve the total energy; additionally, the DNLS model conserves the total norm $\mathcal{S} = \sum_l n_l$. For small amplitudes an approximate mapping, $\beta\mathcal{S} \approx 3WE$, from the KG model to the DNLS model exists [18].

We present analytic results for DNLS and study numerically both models, since it is straightforward to adapt analytics to the KG case. Neglecting the nonlinear terms, Eq.(1) reduces to the linear eigenvalue problem $\lambda A_l = \epsilon_l A_l - (A_{l+1} + A_{l-1})$, in which $A_{\nu,l}$ are the NMs, and $\lambda_\nu \in [-W/2 - 2, W/2 + 2]$ are the NM frequencies in a frequency spectrum width of $\Delta = 4 + W$ [19].

The NM asymptotic spatial decay is given by $A_{\nu,l} \sim e^{-l/\xi(\lambda_\nu)}$ where $\xi(\lambda_\nu)$ is the localization length. It is approximated [20] in the limit of weak disorder ($W \ll 1$) as $\xi(\lambda_\nu) \leq \xi(0) \approx 96W^{-2}$. The NM participation number $P_\nu = 1/\sum_l A_{\nu,l}^4$ characterizes the NM spatial extent. An average measure of this extent is the localization volume V , which is on the order of $3.3\xi(0)$ for weak disorder and unity in the limit of strong disorder [21]. The average frequency spacing of NMs within a localization volume is then $d \approx \Delta/V$. The two frequency scales $d < \Delta$ are thus expected to determine the packet evolution details in the presence of nonlinearity.

Nonlinearity induces an interaction between NMs. The variables $\phi_\nu = \sum_l A_{\nu,l} \psi_l$ determine the complex time-dependent amplitudes of the NMs. Since all NMs are exponentially localized in space, each of them is effectively coupled to a finite number of neighbor modes, i.e. the interaction range is finite. However, the strength of this coupling is proportional to the norm density $n = |\phi|^2$. The frequency shift due to the nonlinearity is then $\delta \sim \beta n$ [19].

The time-dependent normalized norm density distributions in NM space, $z_\nu \equiv n_\nu / \sum_\mu n_\mu$, are tracked for DNLS. The KG counterpart is normalized energy density distributions in NM space. These densities are sorted on the center-of-norm coordinate $X_\nu = \sum_l l A_{l,\nu}^2$, and two measures in NM space used: the participation number $P = 1/\sum_\nu z_\nu^2$ which queries the quantity of strongest excited sites, and the second moment $m_2 = \sum_\nu (\nu - \bar{\nu})^2 z_\nu$ (where $\bar{\nu} = \sum_\nu z_\nu \nu$) which probes distances between a distribution's tail and center. The ratio of the two measures $\zeta = P^2/m_2$ (the compactness index [15]) quantifies the sparsity of a packet - thermalized distributions have $\zeta \approx 3$, while $\zeta \ll 3$ indicates either very sparse packets, or partial self-trapping.

We consider compact wave packets at $t = 0$ spanning a width L centered in the lattice, such that within L there is a constant norm density of n and a random phase at each site (outside the volume L the norm density is zero). In the KG case, this equates to exciting each site in the width L with the same energy density, $\mathcal{E} = E/L$, i.e.

initial momenta of $p_l = \pm\sqrt{2\mathcal{E}}$ with randomly assigned signs.

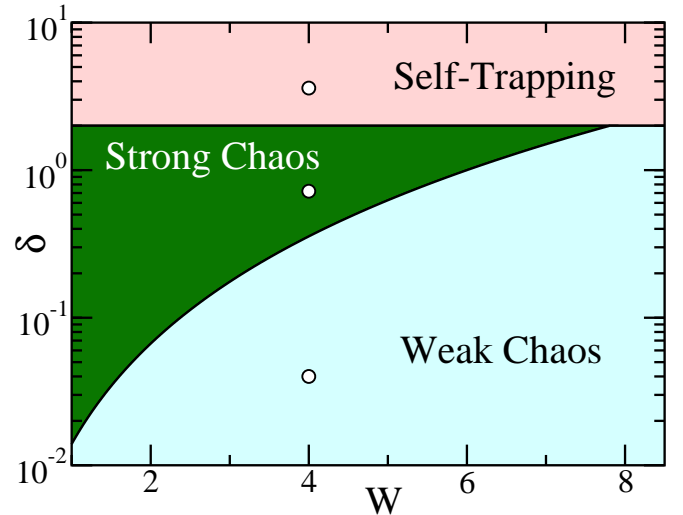


FIG. 1: (Color online) Parametric space of disorder, W , vs. the frequency shift induced by nonlinearity, δ , for the DNLS model. The KG analog is obtained by the small amplitude mapping $\delta \rightarrow 3W\delta$. Three spreading regimes are shown for dynamics dictated by: (i) weak chaos (pale blue), (ii) strong chaos (green), and (iii) the onset of self-trapping (pale red). The three circles show numerical values used in Fig. 2.

For $\beta = 0$ and $L < V$, the packet will extend over V during the time $\tau \sim 2\pi/d$; after that, AL stops further spreading, with a lowered norm density $n(\tau) \approx (nL)/V$. For $L > V$, the norm density will not change appreciably up to τ , so $n(\tau) \approx n$. Let us increase β . The nonlinear frequency shift $\delta = \beta n(\tau)$ should be now compared with the average spacing d . If $\beta n(\tau) < d$, most of the NMs are weakly interacting with each other; hence, this regime is dubbed “weak chaos”. Once $\delta = d$, the NM frequency renormalization begins to allow some NMs interact resonantly, i.e. strongly, with each other. If $\beta n(\tau) > d$, almost all NMs in the packet are resonantly interacting. This regime will be coined “strong chaos”. Note that a spreading wave packet which is launched in the regime of strong chaos will increase in size, drop its norm (energy) density, and therefore cross over into the asymptotic regime of weak chaos at later times. If $\delta \geq \Delta$, a substantial part of the wave packet will be self-trapped. This is due to the occurrence of a wave packet frequency shifting out of resonance with the finite-width linear spectrum. In fact, partial self-trapping will occur already for $\delta \geq 2$ since at least some sites in the packet may be tuned out of resonance. For a single-site excitation $L = 1$ the strong chaos regime shrinks to zero width and one is left only with either weak chaos or self-trapping [11, 12, 14, 15]. **The key distinction of the multiple-site excitations is that they can spread in the strong chaos regime.** Fig. 1 summarizes the predicted regimes in a parametric space for the case $L = V$, in which lines rep-

represent the regime boundaries $\delta = d$ and $\delta = 2$. Note that we used $d = \Delta/(3.3\xi(0))$ with $\xi(0) = 96W^{-2}$ being the weak disorder estimate. More sophisticated numerical estimates of d [21] yield only slight corrections to Fig. 1 for $W > 6$. The weaker the strength of disorder, the larger the window of strong chaos in Fig. 1. Inversely, for $W \geq 8$ the strong chaos window closes almost completely. Ideally, we should utilize the smallest possible value of W , however computational restrictions limit this value; we will choose a reference value of $W = 4$ [22].

In order to observe the crossover, we use $L = 21$ (which is approximately equal to V for $W = 4$) in system sizes of 1000–2000 sites. For DNLS, an initial norm density of $n = 1$ is used, so that $\delta = \beta$. Nonlinearities (\mathcal{E} for KG) are chosen within the three spreading regimes (see Fig. 1), respectively $\beta \in \{0.04, 0.72, 3.6\}$ and $\mathcal{E} \in \{0.01, 0.2, 0.75\}$. Equations (2,4) are time evolved using SABA-class split-step symplectic integration schemes [23], with time-steps of $dt \sim 10^{-2} - 10^{-1}$ up to a maximum $t \sim 10^7 - 10^9$. Conservations are found to be accurate within 1%.

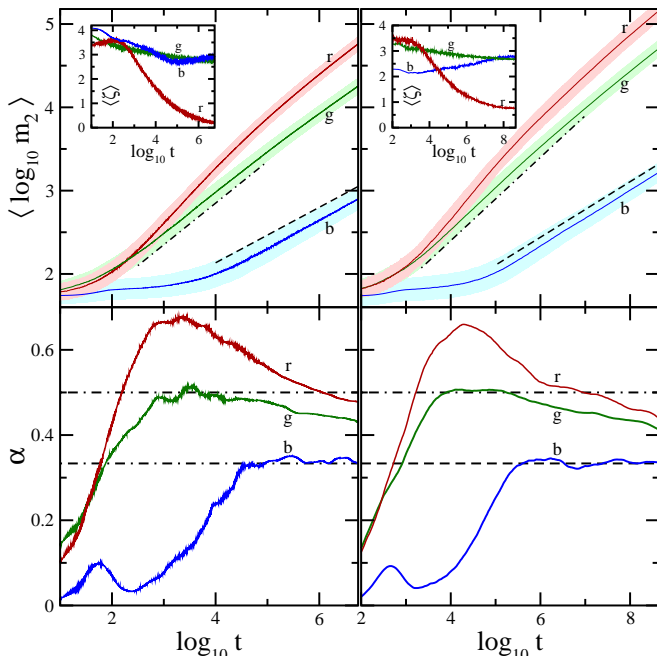


FIG. 2: (Color online) Upper row: Average log of second moments (inset: average compactness index) vs. log time for the DNLS (KG) on the left (right), for $W = 4, L = 21$. Colors/letters correspond the three different regimes: (i) weak chaos - (b)lue, $\beta = 0.04$ ($\mathcal{E} = 0.01$), (ii) strong chaos - (g)reen, $\beta = 0.72$ ($\mathcal{E} = 0.2$), (iii) self-trapping - (r)ed, $\beta = 3.6$ ($\mathcal{E} = 0.75$). The respective lighter surrounding areas show one standard deviation error. Dashed lines are to guide the eye to $\sim t^{1/3}$, while dotted-dashed guides for $\sim t^{1/2}$. Lower row: Finite difference derivatives for the smoothed m_2 data respectively from above curves.

Ensemble averages over disorder were calculated for 1000 realizations and are shown in Fig. 2 (upper row). In

the regime of weak chaos we find a subdiffusive growth of m_2 at large times according to $m_2 \sim t^\alpha$, $\alpha \leq 1$, with a compactness index $\zeta \approx 3$. In the regime of strong chaos we observe a faster subdiffusive growth of m_2 , with an additional slowing down at larger times, as expected from the predicted crossover. The compactness index is also $\zeta \approx 3$, as in the weak chaos regime. Finally, in the regime of partial self-trapping m_2 grows, but the compactness index ζ decreases in time substantially. This indicates that a part of the wave packet is arrested, and another part is spreading.

In order to quantify our findings, we smooth $\langle \log m_2 \rangle$ with a locally weighted regression algorithm [24], and then apply a central finite difference to calculate the local derivative

$$\alpha(\log t) = \frac{d\langle \log m_2 \rangle}{d \log t}. \quad (5)$$

The outcome is plotted in the lower row in Fig. 2.

In the weak chaos regime the exponent $\alpha(t)$ increases up to $1/3$ and stays at this value for later times. In the strong chaos regime $\alpha(t)$ first rises up to $1/2$, keeps this value for one decade, and then drops down, as predicted. Finally, in the self-trapping regime, we observe an even larger rise of $\alpha(t)$.

Following the analysis in [17], the modes inside the packet interact in a nonintegrable way leading to chaotic dynamics. The norm (energy) diffusion is characterized by a diffusion rate $D \sim \beta^2 n^2 (\mathcal{P}(\beta n))^2$, where $\mathcal{P}(\beta n) \approx 1 - e^{-\beta n/d}$ is the probability of packet modes to resonate [17, 21]. From $m_2 \sim 1/n^2$ and the diffusion equation $m_2 \sim Dt$, one obtains an equation $1/n^2 \sim \beta(1 - e^{-\beta n/d})t^{1/2}$ that determines the subdiffusive spreading crossover from the regime of strong chaos to that of weak chaos

$$m_2 \sim \begin{cases} \beta t^{1/2}, & \beta n/d > 1 \text{ (strong chaos)} \\ d^{-2/3} \beta^{4/3} t^{1/3}, & \beta n/d < 1 \text{ (weak chaos)} \end{cases} \quad (6)$$

The origin of the strong chaos regime is now easily seen; $\mathcal{P} \approx 1$ if βn is sufficiently larger than d . Such a situation can be generated for packets with large enough βn (or energy density \mathcal{E} for KG) in which every mode in the packet resonates, and the condition for strong chaos yields faster spreading, $m_2 \sim t^{1/2}$. These predictions for strong chaos are then observed at $t \sim 10^3 - 10^4$ (KG: $10^4 - 10^5$) in Fig. 2; time averages in these regions over the green curves yield $\alpha \approx 0.49 \pm 0.01$ (KG: 0.51 ± 0.02).

With spreading continuing in the strong chaos regime, the norm density in the packet will decrease, and eventually $\beta n \leq d$. Then a dynamical crossover occurs to the slower weak chaos subdiffusive spreading. This crossover spans logarithmic time scales. Nevertheless, in the green curves of Fig. 2 a clear decay in α to values below $1/2$ is observed. Fits of the decay further suggest $\alpha \approx 1/3$ at $t \sim 10^{10} - 10^{11}$. The challenge remains to directly

observe saturation at times accessible in computational experiments.

In the regime of self-trapping, a good portion of the excitation remains highly localized, while the remainder spreads (red curves in Fig. 2). Therefore, P does not grow significantly, but the second moment does. Consequently, ζ drops and is a good indicator of the degree of self-trapping. The time evolution of ζ for excitations in different regimes is shown in the insets of Fig. 2. In the regimes of weak and strong chaos, if self-trapping is avoided, the compactness index at largest computational times is $\zeta \approx 2.85 \pm 0.79$ (KG: 2.74 ± 0.83), as seen in the blue and green curves of Fig. 2. This means that the wave packet spreads, but remains thermalized ($\zeta \approx 3$). For the self-trapping regime (red curves), the compactness index asymptotically decreases to very small values. Note in Fig. 2 at intermediate times, there is transient growth where $\alpha > 1/2$; nonetheless it remains subdiffusive ($\alpha < 1$). At larger times, this overshoot decreases. This is presumably due to some self-trapped states which interact strongly with the spreading part of the packet and release their norm (energy) into the thermal cloud at some time. These more complicated scenarios are not yet quantitatively understood, and certainly remain for future exploration.

This crossover can be expected to show up in measurements of the heat conductivity κ at finite norm (energy) densities. According to the heat equation $\partial T(x, t)/\partial t = \kappa/c\partial^2 T/\partial x^2$ where T is the temperature and c the specific heat. Therefore the heat conductivity is proportional to the diffusion rate $\kappa = cD$. For small norm (energy) densities, heat is proportional to the densities. Therefore we expect that for $\beta n > d$, i.e. in the regime of strong chaos, $\kappa \sim T^2$ (here T is the temperature). For small enough temperatures one crosses over into the regime of weak chaos, and consequently we expect $\kappa \sim T^4$.

Let us summarize. In the presence of nonlinearity within one-dimensional disordered systems, Anderson localization is destroyed. In this Letter, we use a novel technique of ensemble averaging and local derivatives on logarithmic scales. In contrast to previous results for single site excitations, we find that multiple site excitations can evolve either in the asymptotic regime of weak chaos, or in an intermediate regime of strong chaos (excluding self-trapping for strong nonlinearities). In the weak chaos regime the second moment m_2 grows subdiffusively as $t^{1/3}$. In the strong chaos regime subdiffusion is faster, yielding $m_2 \sim t^{1/2}$, with a subsequently slow (on logarithmic time scale) crossover to an asymptotic weak chaos law.

The authors wish to thank S. Aubry, S. Fishman, N. Li, R. Khomeriki, & A. Pikovsky for insightful discussions.

- [1] P. Anderson, *Phys. Rev.* **109**, 1492 (1958).
- [2] D. S. Wiersma, et al., *Nature* **390**, 671 (1997); H. Cao, et al., *Phys. Rev. Lett.* **82**, 2278 (1999); A. A. Chabanov, M. Stoytchev, & A. Z. Genack, *Nature* **404**, 850 (2000); H. Cao, *Waves in random media* **13**, 1 (2003); M. Störzer, et al., *Phys. Rev. Lett.* **96**, 063904 (2006).
- [3] R. L. Weaver, *Wave Motion* **12**, 129 (1990); H. Hu, et al., *Nat. Phys.* **4**, 945 (2008).
- [4] R. Dalichaouch, et al., *Nature* **354**, 53 (1991); C. Dembowski, et al., *Phys. Rev. E* **60**, 3942 (1999); J. D. Bodyfelt, et al., *Phys. Rev. Lett.* **102**, 253901 (2009).
- [5] T. Schulte, *Acta Phys. Polon. A* **109**, 89 (2006); G. Roati, et al., *Nature* **453**, 895 (2008).
- [6] T. Pertsch, et al., *Phys. Rev. Lett.* **93**, 053901 (2004); T. Schwartz, et al., *Nature* **446**, 52 (2007); Y. Lahini, et al., *Phys. Rev. Lett.* **100**, 013906 (2008).
- [7] J. Billy, et al., *Nature* **453**, 891 (2008); L. Sanchez-Palencia & M. Lewenstein, *Nat. Phys.* **6**, 87 (2010).
- [8] S. A. Gredeskul & Y. S. Kivshar, *Phys. Rep.* **216**, 161 (1992); T. Kottos & M. Weiss, *Phys. Rev. Lett.* **93**, 190604 (2004); T. Paul, et al., *Phys. Rev. A* **72**, 063621 (2005); *Phys. Rev. Lett.* **98**, 210602 (2007).
- [9] J. Fröhlich, T. Spencer, & C. E. Wayne, *J. Stat. Phys.* **42**, 247 (1986); G. Kopidakis & S. Aubry, *Phys. Rev. Lett.* **84**, 3236 (2000); S. Fishman, A. Iomin, & K. Mallick, *Phys. Rev. E* **78**, 891 (2008); J. D. Bodyfelt, T. Kottos, & B. Shapiro, *Phys. Rev. Lett.* **104**, 164102 (2010).
- [10] D. Shepelyansky, *Phys. Rev. Lett.* **70**, 1787 (1993); B. Shapiro, *Phys. Rev. Lett.* **99**, 060602 (2007); S. E. Skipetrov, et al., *Phys. Rev. Lett.* **100**, 165301 (2008).
- [11] A. S. Pikovsky & D. L. Shepelyansky, *Phys. Rev. Lett.* **100**, 094101 (2008).
- [12] H. Veksler, Y. Krivolapov & S. Fishman, *Phys. Rev. E* **80**, 037201 (2009).
- [13] G. Kopidakis, et al., *Phys. Rev. Lett.* **100**, 084103 (2008).
- [14] S. Flach, D.O. Krimer, & Ch. Skokos, *Phys. Rev. Lett.* **102** (2009);
- [15] Ch. Skokos, et al., *Phys. Rev. E* **79**, 056211 (2009);
- [16] Ch. Skokos & S. Flach, arXiv:condmat/1001.5171 (2010).
- [17] S. Flach, *Chem. Phys.*, in press (2010).
- [18] Y. S. Kivshar & M. Peyrard, *Phys. Rev. A* **46**, 3198 (1992); Y. S. Kivshar, *Phys. Rev. E* **48**, 4132 (1993); M. Johansson, *Physica D* **216**, 62 (2006).
- [19] KG model (3) is reduced to the linear eigenvalue problem with $\epsilon_l = W(\tilde{\epsilon}_l - 1)$ and $\lambda_\nu = W\omega_\nu^2 - W - 2$. The width of squared eigenfrequencies $\omega_\nu^2 \in [1/2, 3/2 + 4/W]$ spectrum is $\Delta = 1 + 4/W$. The nonlinear frequency shift due to small amplitude DNLS \rightarrow KG mapping is $\sim \delta/3W$.
- [20] B. Kramer & A. MacKinnon, *Rep. Prog. Phys.* **56**, 1469 (1993).
- [21] D.O. Krimer & S. Flach, in preparation (2010).
- [22] We have also performed numerics for $W = 6, L = V = 11$. Results are qualitatively identical to those shown in Fig. 2, therefore we have omitted them for the sake of graphical clarity.
- [23] J. Laskar & P. Robutel, *Celest. Mech. Dyn. Astron.* **80**, 39 (2001).
- [24] W. S. Cleveland & S. J. Devlin, *J. Amer. Stat. Assoc.* **83**, 596 (1988).

* Electronic address: lapteva@pks.mpg.de